Tuning the Elastic Modulus of Hydrated Collagen Fibrils

Colin A. Grant,[†] David J. Brockwell,[†] Sheena E. Radford,[†] and Neil H. Thomson[†‡*]
[†]Astbury Centre for Structural Molecular Biology, Institute of Molecular and Cellular Biology, and [‡]Molecular and Nanoscale Physics, School of Physics and Astronomy, University of Leeds, Leeds, United Kingdom

ABSTRACT Systematic variation of solution conditions reveals that the elastic modulus (*E*) of individual collagen fibrils can be varied over a range of 2–200 MPa. Nanoindentation of reconstituted bovine Achilles tendon fibrils by atomic force microscopy (AFM) under different aqueous and ethanol environments was carried out. Titration of monovalent salts up to a concentration of 1 M at pH 7 causes *E* to increase from 2 to 5 MPa. This stiffening effect is more pronounced at lower pH where, at pH 5, e.g., there is an ~7-fold increase in modulus on addition of 1 M KCl. An even larger increase in modulus, up to ~200 MPa, can be achieved by using increasing concentrations of ethanol. Taken together, these results indicate that there are a number of intermolecular forces between tropocollagen monomers that govern the elastic response. These include hydration forces and hydrogen bonding, ion pairs, and possibly the hydrophobic effect. Tuning of the relative strengths of these forces allows rational tuning of the elastic modulus of the fibrils.

INTRODUCTION

Biomechanically speaking, collagen is the most important protein to the human body. In one form or another, collagen-based materials are found in vital tissues and structures that sustain our locomotion. In the skeletal system, which gives the human form its basic rigidity and protects the major organs, collagen is the major constituent of the organic matrix of bone. Other examples of biomechanically important tissues that contain collagen are tendons, ligaments, skin, and cartilage. Since collagen has a fibrillar and ropelike structure (1), it is an interesting biocompatible material for biomedical and new materials applications, ranging from tissue engineering scaffolds (2) to nanomechanics (3). In tissue-engineered scaffolds, cells are responsive to the microenvironment in which they reside (4); therefore, being able to fine-tune the mechanical properties of collagen-based scaffolds could be important for controlling mechanotransduction and possibly differentiation of stem cells (5). This study describes how the elastic properties of individual collagen fibrils can be altered in vitro through change of the surrounding solution properties.

Monomeric collagen has a molecular structure that is comprised of a triple helix of left-handed polypeptide chains that come together to form a right-handed twisted molecule known as tropocollagen. Type I collagen contains two $\alpha 1$ chains and one $\alpha 2$ chain, each containing ~1000 amino acid residues. Each chain is staggered relative to the others by one amino acid residue, and these are twisted together to form the triple-helical tropocollagen monomers that make up the larger-diameter fibrils (6). The dimensions of the monomer are diameter ~15 Å and length ~300 nm, and these monomers self-assemble into a staggered cross-striated fibrillar arrangement with a periodic banding of 67 nm (7). Recent mechanical manipulation experiments with atomic force microscopy (AFM) combined with imaging, demonstrate that contrary to established models (8), collagen fibrils are made up of tropocollagen molecules that are twisted together to form ropes with nanoscale diameters (1).

The generalized well-known formula for collagen amino acid sequence is Gly-*X*-*Y*, where *X* is predominantly proline (Pro) and *Y* a hydroxyproline (Hyp) residue (9). Glycine, which occurs at every third residue, is found at the center of the coiled peptide chain to allow a close packing of the triple helix. In tropocollagen monomers, 12% of tripeptides have the sequence Gly-Pro-Hyp, whereas ~44% have sequences of Gly-Pro-*Y* and Gly-*X*-Hyp, and the remaining 44% is made up of Gly-*X*-*Y* containing no amino acids (10). Charged residues such as lysine, arginine, glutamic acid, and aspartic acid make up ~15–20% of all residues in the tropocollagen monomer, and ~40% of Gly-*X*-*Y* sequences contain at least one charged residue (6). Therefore, electrostatic interactions are thought to be of great importance for the stability of the triple-helical conformation with tropocollagen (6,11). In fact, there could be as many as 500 possible intermolecular side-chain interactions along the collagen triple helix (12). However, because the number of charged residues in the tropocollagen molecule is large, it is difficult to measure and quantify each individual interaction (6).

Development of local-force probe techniques, such as AFM, in recent years allows localized mechanical measurements to be made on the nanometer scale, such that individual collagen fibrils can be directly tested (13–19). Although the distribution of fibril diameters is large, from 20 nm in cornea to up to ~500 nm in mature tendon (20), collagen fibrils of all sizes are suitable for measuring by nanoindentation. Provided that the fibril diameter is larger than the diameter of the end of the AFM tip, relatively simple contact mechanics models, such as those derived from Hertz

Submitted April 27, 2009, and accepted for publication September 3, 2009.

*Correspondence: n.h.thomson@leeds.ac.uk

Editor: Elliot L. Elson.

0006-3495/09/12/2985/8 $2.00

doi: 10.1016/j.bpj.2009.09.010

(21), can be used to extract elastic modulus from force-indentation data. Hertzian contact theory is readily applied to AFM force/indentation plots and can provide modulus estimations of biological samples (22–27). Recently, collagen fibrils have been mechanically probed using AFM by Heim et al. (15) and Wenger et al. (17), giving modulus ranges of 1–2 GPa and 5–11.5 GPa, respectively, in ambient conditions. Other work on the collagen fibril modulus in air has been carried out by Strasser et al. (28), who indented and dissected intact fibrils, reporting no change in modulus between the shell and the core of the native fibrils. The data do, however, show an increase in the adhesion between the AFM probe and the core region of a microdissected collagen fibril.

Studies have shown that hydrated collagen fibrils under bulk aqueous solution conditions, which are more closely related to the situation in vivo, experience a reduction in modulus compared to the anhydrous form. These reductions are ~2–3 orders of magnitude: in three-point bending (18,29), the bending modulus reduced from 1–4 GPa to 70 MPa; during tensile testing (16), the tensile modulus reduced from 2–7 GPa to 200–800 MPa, and through nanoindentation (13), the compressive modulus reduced from 1–2 GPa to 1–2 MPa. It has been suggested that under neutral pH buffer conditions, the monomeric collagen molecules are not solely responsible for the elasticity, that the interaction of the tropocollagen with the fluid phase within the fibril is a significant contributor (13). This idea is corroborated by other AFM experimentation that shows that the measured hydrated shear modulus changes very little when a cross-linker is applied to collagen fibrils (18).

This article highlights the range of elastic response of collagen type I fibrils that can be achieved in liquid by altering the environment. Here, we discuss the finding that the mechanical properties of hydrated collagenous fibrils can be tuned by adding salts, by changing the solution pH, or by changing the solvent. With collagen such a crucial protein in biomechanical tissues, and its use in tissue-engineering scaffolds (30,31), the fact that the nanomechanical compressive modulus can be significantly altered, and indeed strengthened, has important implications for biomaterial applications of collagen fibrils.

MATERIALS AND METHODS

Collagen fibril deposition

Collagen fibrils for this study were isolated from bovine Achilles tendon (Sigma Aldrich, St. Louis, MO) and were prepared according to the method of van der Rijt et al. (16). In short, the tendon was dissolved in 10 mM HCl, homogenized using a hand blender, and then diluted 150 times in sodium phosphate buffer (100 mM, pH 7). Silica wafers and gold-coated silica wafers were cleaned in a surfactant solution (Decon 90, Decon Laboratories, Haan, Germany), rinsed in excess MilliQ water (Millipore, Billerica, MA) (18 MΩ cm), then dried in nitrogen. A droplet (~20 μL) of collagen solution was placed on the surface of a wafer for 20 min, after which the wafer was rinsed in pure water and gently dried in a stream of nitrogen before being immersed in the test liquid environment. A fresh sample of adsorbed collagen fibrils was used for each separate medium condition.

AFM and nanoindentation

AFM imaging and force measurements were made using silicon nitride cantilevers with integral tips (Applied Nanostructures, Santa Clara, CA) with spring constants of the order $k \sim 0.3$ N/m on an MFP-3D AFM (Asylum Research, Santa Barbara, CA). A closed fluid cell was used so that the surfaces with adsorbed fibrils were totally immersed in 2 mL of solution for 1 h before scanning and indenting. For this study, only fibrils between 80 and 200 nm in height were mechanically tested, as Heim et al. (15) report that no size-dependent modulus variation was detected in this range.

Force volume (FV) imaging was carried out on isolated fibrils using arrays of 50 × 50 pixels, with each pixel representing a single force-distance measurement. A tip velocity of 600 nm/s was used throughout (scan rate, 1 Hz; height above surface, 300 nm), and the maximum force threshold was not taken above values that induced any more than 40% indentation strain. Strain was defined as the fibril indentation over the measured height in the AFM tapping-mode images. The calculated modulus of collagen fibrils does not change at loading rates up to 1500 nm/s (data not shown).

Tapping-mode scans were taken before FV imaging to locate a suitable fibril, and afterward to ensure that the force measurements did not permanently deform the fibril. The built-in software of the MFP-3D is used to calculate both the cantilever spring constant, which uses the thermal tuning method (32), and the reduced elastic modulus (E_r), which uses a Hertzian contact theory (Eq. 1),

$$E_r = \frac{3F(1-\upsilon^2)}{4\sqrt{R_e}}\delta^{-3/2}, \quad (1)$$

where F is the applied load, ν is the Poisson ratio (taken as 0.5), R_e is the reduced radius of contact ($1/R_e = 1/R_{tip} + 1/R_{fibril}$), which takes into consideration the spherical tip radius and cylindrical fibril radius, and δ is the indentation depth. Equation 1 can be used for a spherical or a parabolic probe. In fact, after the indentation of gelatin films, the prediction of the spherical/parabolic Hertz model matched the experimental data over a wide indentation range up to 5 R_{tip} (33). The value for R_{tip} was fixed at 15 nm for this study, based on the manufacturer's quoted value at 15 nm or less. This limit was confirmed through high-resolution imaging of structures smaller than this, such as amyloid fibrils with diameters of 5–10 nm. The value for R_{fibril} is taken as half the maximum height from the line section of the fibril that undergoes FV analysis. An increase of R_{fibril} from 75 to 100 nm results in a change in modulus of only 1.4%.

To measure the elastic modulus under compression, only those force/indentation plots extracted from the central axis of the collagen fibril are used, to avoid artifacts due to geometric effects between the curved fibril and the nanosized tip. As the fibril is elliptical or cylindrical in cross section, it is likely that indents at its edge will be a combination of indentation of the collagenous material and free space. The number of extracted curves/FV for modulus analysis is in the region of 100. All plotted data are shown as the mean ± SD of the histograms of modulus extracted from all pixels in the FV images.

Scanning media

The range of solutions used includes 0–1 M NaCl, KCl, or NH_4Cl in 100 mM sodium phosphate (pH 7) and 0–100% ethanol in 100 mM sodium phosphate (pH 7). To carry out experiments at pH 5, two different potassium acetate buffers of 150 mM and 300 mM with 0–1 M KCl were used to create a range of ionic strengths. It is important to note that the two buffers (100 mM sodium phosphate and 300 mM potassium acetate) have an identical ionic strength even though their pH values are different. Ionic strength was deduced using the Henderson-Hasselbalch equation to calculate the concentrations of all the charged species. Freshly prepared collagen samples on silica or gold substrates were immersed in 2 mL of the scanning medium

in a closed fluid cell and then left for 1 h before any mechanical measurements were taken. This time interval was necessary to ensure that equilibration occurred.

RESULTS

Effect of fibril swelling in aqueous buffer

Mechanical measurement of individual collagen fibrils by AFM requires that the fibrils are stably adsorbed to a surface during imaging and nanoindentation. Measurements of the same collagen fibrils physisorbed on a silicon surface in air and in buffer demonstrate that stable AFM imaging can be achieved in liquids (Fig. 1 *A*). In going from air to buffer, the collagen fibrils swell ~2-fold, as seen in the line sections. Collating the average fibril height for several collagen fibrils in a number of solution conditions shows an interesting trend (Fig. 1 *B*). Swelling occurs in the hydrated form but does not change significantly among different conditions of salt and pH. In 100% ethanol, which is hygroscopic, the fibril heights are reduced to values similar to those in air.

The observation of swelling on the same fibrils highlights the importance that hydration plays in the mechanical response. The large reduction in elastic modulus seen between measurements in air compared to aqueous solutions (13,16,18,19) suggests that the collagen fibril mechanics are strongly influenced by the liquid phase of this biocomposite material. The behavior of fibril height and its correlation with measured elastic modulus is discussed later.

It should be pointed out that different imaging modes were used to collect the two scans in Fig. 1 *A*: contact-mode imaging was used in air, whereas tapping mode was used in liquid, with the same cantilever used in both modes. This was necessary to scan the same sample area after introducing liquid into the AFM imaging chamber, as contact mode in liquid produces shearing interactions that disturb reliable imaging of the collagen fibrils. The cantilever used is a low-spring-constant lever ($k \sim 0.3$ N/m), which is appropriate for low imaging forces using contact mode in air and can be driven with sufficiently large amplitude in liquid for tapping-mode imaging. Although there is the possibility that the amount of compression of the collagen fibrils is different in each case, the large increase of the height distributions upon addition of buffer is unlikely to be caused by different ways of loading the fibril, given that the modulus in air is known to be three orders of magnitude higher (13).

Reliable imaging of the collagen fibrils under liquid conditions, and particularly in aqueous environments, allows the effects of changing solution conditions around individual fibrils to be explored. Fig. 2 *A* shows a typical AFM amplitude scan of an individual collagen fibril taken under 100 mM sodium phosphate buffer (pH 7). Amplitude images highlight the banding more than topography, because this data signal is an efficient edge detector and is not low-pass filtered through the electronic feedback loop and the mechanical inertia of the scan piezo. Fig. 2 *B* shows an FV

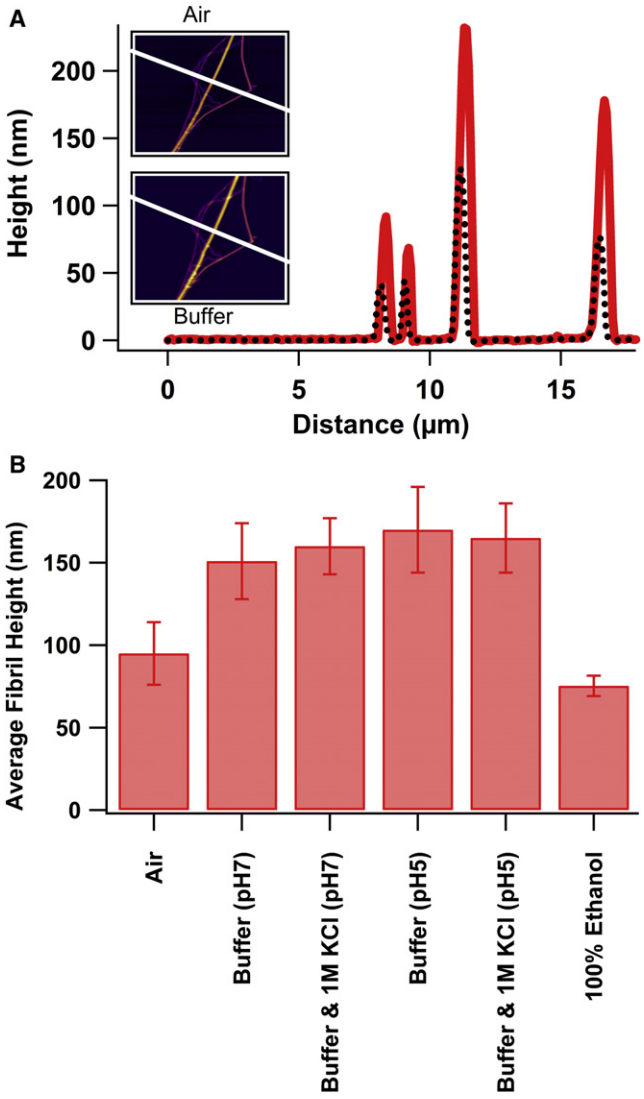

FIGURE 1 (*A*) Line sections of AFM images 20 × 20 μm taken on the same region of the same collagen fibrils in air (*upper inset*) and after 1 h in neutral buffer (*lower inset*). The heights of all fibrils increased by approximately a factor of 2 after 1 h in buffer. Air, dashed line; buffer, solid line. (*B*) Average collagen fibril heights under different conditions, showing that all aqueous conditions cause similar degrees of swelling, whereas 100% ethanol does not.

indentation map, with its corresponding grayscale bar, taken on the same fibril as in Fig. 2 *A* immediately after the scan. Note that lighter regions have a larger recorded indentation. One can see that there is less indentation at the center of the fibril due to the greater thickness and absence of any geometrical edge effect in that area. Typical force curves extracted from the FV map (Fig. 2 *C*) show the difference between indenting hard silica and indenting the collagen fibril. The measured indentation is used to fit the data to the Hertzian contact mechanics and thereby extract a value of Young's modulus (Eq. 1), giving an average value of 2.1 ± 0.4 MPa. Adhesion from some retraction curves (data not shown)

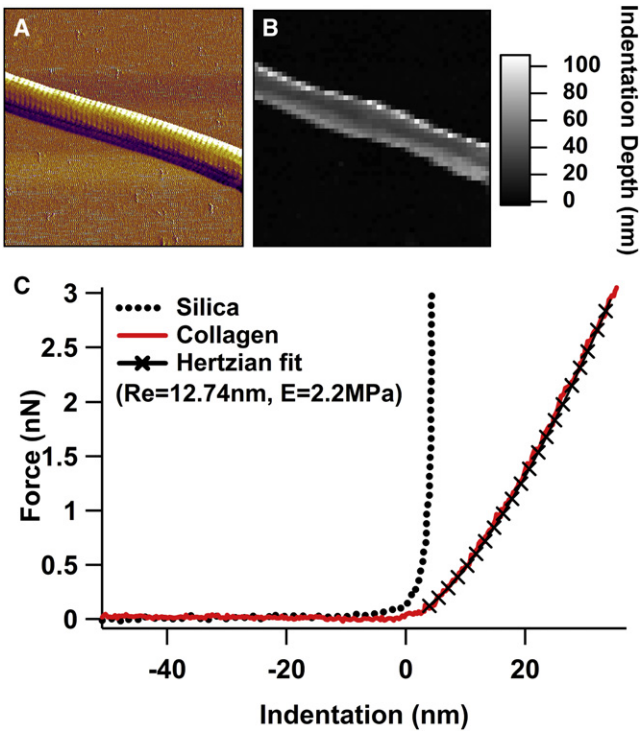

FIGURE 2 (*A*) Tapping-mode residual amplitude (error signal) image (2 × 2 μm) of a hydrated collagen fibril in 100 mM sodium phosphate, pH 7. (*B*) Force volume image (50 × 50 pixels) of a corresponding collagen fibril. (*C*) Two curves extracted from the FV image in *B*, one taken on the hard silica support surface (*dashed line*) and the other on the central axis of the fibril (*solid line*), showing indentation of the collagen. The Hertzian contact mechanics fit is shown (*black crosses*).

counts for ~5% of the loading force and is considered to be negligible.

Effect of salt concentration

To investigate whether changing the solution conditions around collagen fibrils alters their elasticity in a reproducible manner, NaCl was added to the 100 mM sodium phosphate buffer (pH 7) to concentrations up to 1 M. The modulus value showed no appreciable change up to 500 mM NaCl, but a 2.3 times increase in modulus was detected at 1 M NaCl (Fig. 3), with an average value of 4.8 ± 1.3 MPa. Separate, freshly adsorbed collagen samples were used for each of the different salt buffer conditions. Imaging of the fibril in 1 M NaCl showed no noticeable change in the morphology (cf. Figs. 2 *A* and 3), suggesting that this effect was related to subtle changes in the intermolecular interactions of the tropocollagen monomers rather than to gross structural changes.

Effect of altering the cation species

After observing that increased salt concentration caused an effective stiffening of the collagen fibrils, we examined whether these effects are ion-specific or are simply dependent on the total ionic strength. Various monovalent chloride salt solutions were used at concentrations up to 1 M. The cations were chosen to range across the Hofmeister series, where changing ionic species is known to affect protein stability and solubility (34). Fig. 4 demonstrates that the cation species does not influence the final value of elastic modulus at 1 M monovalent chloride salt; therefore, the increase in modulus at higher salt concentration appears to be related to the ionic strength of the solution surrounding the collagen.

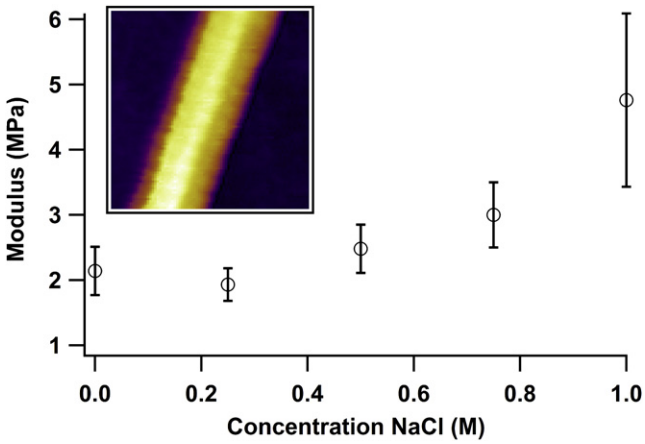

FIGURE 3 Increase of the elastic modulus of collagen fibrils as a function of NaCl concentration. (*Inset*) AFM height image (700 × 700 μm) of a collagen fibril in 100 mM sodium phosphate (pH 7) containing 1 M NaCl, showing the expected D-banding.

To ensure that the changes we observed in the modulus reflect internal changes in the collagen fibrils and do not result from alteration of the interaction between the fibrils and the supporting surface, the support substrate was changed from silicon to gold and several of the measurement conditions were repeated. Within error, the measured modulus was identical whether the fibrils are adhered to silicon or gold, when measured in air or in 100 mM sodium phosphate buffer (pH 7), and with or without 1 M KCl (data not shown).

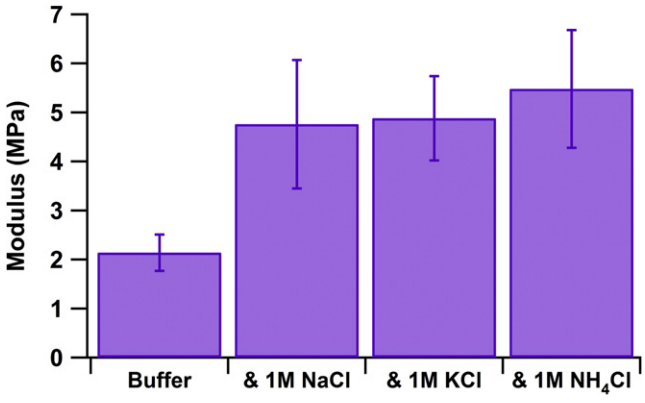

FIGURE 4 Modulus of collagen fibrils in 100 mM sodium phosphate buffer (pH 7) with various monovalent chloride salts added to a concentration of 1 M.

Effect of lowering pH

To further investigate how interactions of electrostatic origin affect the compressive modulus of hydrated collagen fibrils, the effect of pH on Young's modulus was also measured. Force plots taken in 300 mM potassium acetate buffer at pH 5 showed that the effect on the modulus of adding salt (1 M KCl) was greatly enhanced when the pH was lowered (Fig. 5 *A*). The modulus with no added salt in 300 mM potassium acetate buffer (pH 5) was 3.1 ± 0.5 MPa, slightly higher than that in 100 mM sodium phosphate (pH 7). These buffers have equivalent ionic strength, suggesting that this small, but significant, change is due solely to the pH change. After the addition of 1 M KCl at pH 5, there was a dramatic (sevenfold) increase in modulus to 22.3 ± 6.7 MPa. The combined effects of lowering pH to 5 and increasing salt concentration to 1 M raises the modulus by 10-fold compared with its value at pH 7 with no salt (Fig. 5 *B*). Increasing the ionic strength gradually through the use of two different potassium acetate buffers (150 mM and 300 mM), and increasing amounts of KCl, gave a gradual increase in the measured modulus (Fig. 6).

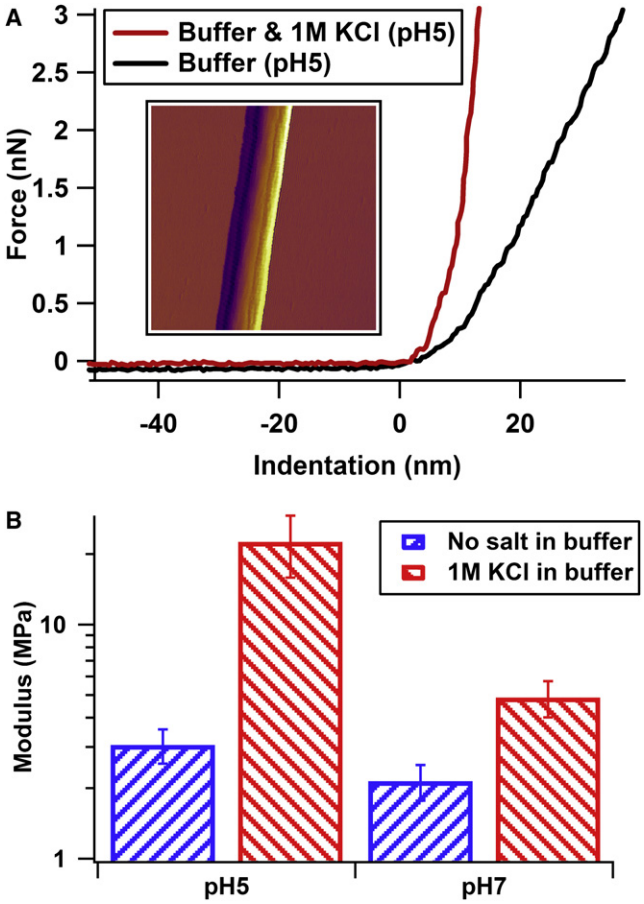

FIGURE 5 (*A*) Typical extracted force-indentation plots made in the presence and absence of 1 M KCl, showing the stiffening effect of the salt. (*Inset*) Tapping-mode amplitude image (2 × 2 μm) of a collagen fibril in 300 mM potassium acetate (pH 5) with 1 M KCl added. (*B*) Comparison of the modulus change after the addition of 1 M KCl to each buffer at pH 5 and pH 7.

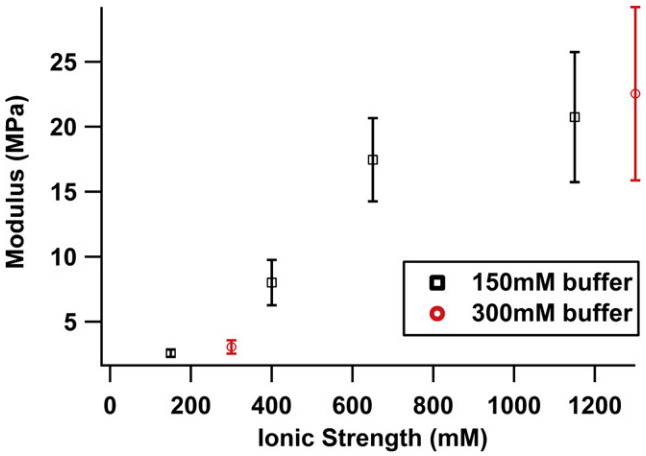

FIGURE 6 Gradual increase in measured modulus with increasing ionic strength from the use of two different potassium acetate buffers (150 mM and 300 mM) and increasing amounts of KCl.

Effect of ethanol

Since large changes in the modulus were observed by altering the ionic composition and strength of aqueous media, we next investigated the effect of changing the surrounding liquid to a nonaqueous medium. Freshly prepared collagen fibril samples were placed under an increasing concentration of ethanol in 100 mM sodium phosphate (pH 7) and their elastic modulus was determined (Fig. 7 *A*). Under these conditions, the modulus steadily increases with increasing ethanol concentration up to 50% (v/v). Thereafter, a large increase in modulus, to $E = 172.5 \pm 59$ MPa, was found when the scanning medium was increased to 100% ethanol. It was necessary to increase the applied force to 50 nN at 100% ethanol (Fig. 7 *B*), as the previously used 3-nN threshold was insufficient to get any measurable indentation in the collagen fibril. The indentation depths measured from the FV analysis in 100% ethanol are lower than those measured in buffer; hence, the standard deviation in the measured modulus is larger. Even though a large increase in modulus is recorded, there is no physical change in the periodic banding in the fibril or in overall fibril morphology (*inset*, Fig. 7 *A*).

DISCUSSION

We have presented an empirical study that shows the effect of changing solution properties on the elastic response. Changing from dehydrated conditions in air to hydrating aqueous solutions causes osmotically driven swelling of the fibrils, as water penetrates the structure. This leads to a drop in the elastic modulus of two or three orders of magnitude (13,16,18). In a hygroscopic liquid, like ethanol, the fibrils behave comparably to the dehydrated state in air. Mixtures of ethanol in buffer give intermediate values of

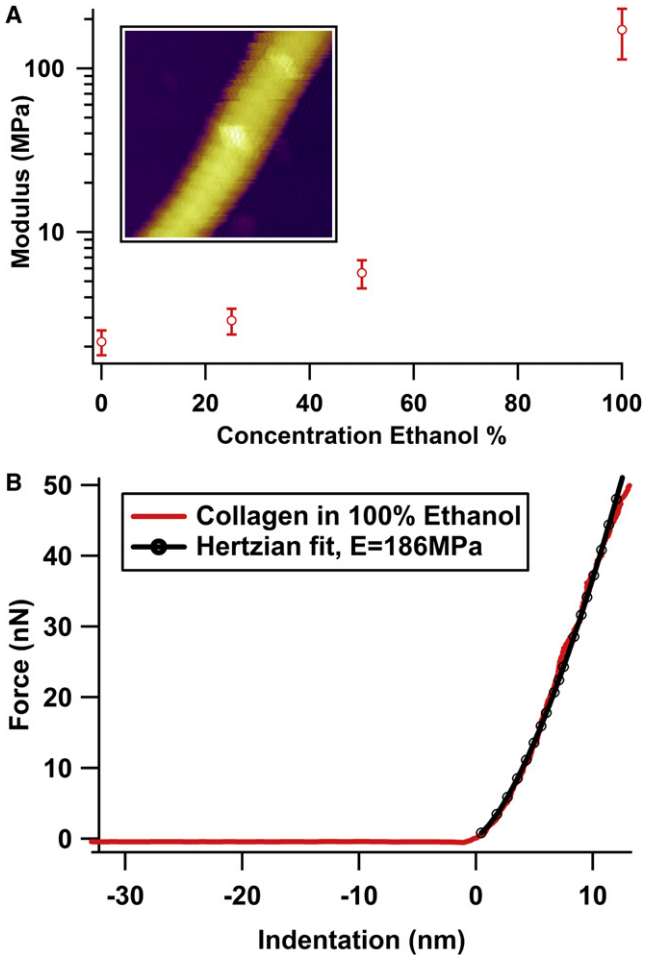

FIGURE 7 (*A*) Change of modulus of collagen fibrils in increasing concentrations of ethanol in 100 mM sodium phosphate buffer. (*Inset*) Tapping-mode image (700 × 700 nm) taken in 100% ethanol. (*B*) Typical force plot made in 100% ethanol, with Hertzian fitting.

elastic modulus, and exchanges between solutions indicate that these effects are reversible (data not shown). Although differences in modulus among fibrils in aqueous and those in alcoholic media can simply be thought of in terms of an osmotic effect, interpreting the modulus changes in different aqueous solutions is difficult due to the complexity of the collagen structure. Consequently, a variety of different molecular interactions occur, and it is difficult to definitively assess a single type of intermolecular interaction as the major contributor to these modulus changes. The modulation of the elastic response of the fibrils in conditions where liquid molecules in the collagen are not being exchanged with the external solution must arise from changes in intermolecular interactions among neighboring tropocollagens. Repulsive forces can arise from electrostatic repulsion and repulsive hydration forces, whereas attractive forces can be contributed from van der Waals, hydrogen bonding, ion pairs (electrostatic attraction), hydration forces, counterion correlation forces and the hydrophobic interaction. The changes in modulus as ionic strength goes up and pH goes down presumably arise from a strengthening of the attractive force components (since the repulsive electrostatic interaction is not greatly modified; see below). We now discuss the origins of the major contributions and their likely magnitude.

Electrostatic interactions

The fact that the average fibril height remains within the same range over all the aqueous solutions we studied (Fig. 1 *B*) indicates that the amount of water retained within the fibrils is the same, and that any changes in intermolecular separation among neighboring tropocollagen molecules is small by comparison. The intermolecular spacing among tropocollagens has been measured at 0.12–0.2 nm, depending on solution conditions (35,36). The Debye length at the highest salt conditions we tested (e.g., 1 M NaCl) is ~0.3 nm (37), and it becomes very much longer at lower concentrations. This would suggest that once assembled, electrostatic repulsion between like-charged residues in the collagen fibril plays a minor role; however, screening of charge-charge interactions is important for the collagen self-assembly process (6).

The most difficult trend to rationalize in our study is the augmentation of the elastic modulus in response to lowering of the pH and in particular the larger increase in the modulus when salt is added. This observation indicates that better screening of charged residues and formation of specific interactions, such as salt bridges, between charged residues leads to stabilization of collagen (38) and collagenlike triple-helical peptides (6). However, Leikin et al. noted a weakening of attraction (i.e., larger separation) between tropocollagen molecules when the pH was lowered on their collagen films prepared from rat tail tendon (35).

The isoelectric points of various collagens have not been extensively characterized to date, and in our case they are unknown, but measurements of collagen from bovine dermal samples indicate that isoelectric points could be above pH 9 (38). However, the acid-base behavior of collagen type I fibrils is strongly influenced by the ionic strength of KCl (38), making predications on the charge state of collagen in particular solvent conditions difficult. In general, however, stability goes up as pH decreases (39), suggesting increased ionization and a role of ion pairs in stabilization. It is probable; therefore, that lowering the pH will increase the overall charge on the system and lead to a more positively charged fibril enhancing salt-bridging effects by increasing polarization.

Hydration forces

Water ordering around hydrophobic residues is thought to have a strong influence on protein structure and stability, at least for globular protein systems (40). However, for extended macromolecular assemblies, such as collagen, DNA, and lipid bilayers, ordering of water around hydrophilic groups may be more dominant. Studies by Leikin

et al. have led to suggestions that hydration forces dominate the tropocollagen interactions at their short separations, whereas van der Waals and electrostatic effects are negligible. An osmotic stress technique (36) on collagen films made from rat tail tendon combined with x-ray diffraction allowed the intermolecular spacing to be directly correlated to the osmotic force applied (35,36,41). For these collagen films the hydrophobic interaction was found to be negligible and water-mediated hydrogen bonding between polar residues was suggested to be the dominating interaction (35). Addition of monovalent salt (NaCl) to a concentration of 1 M was found to decrease in the average spacing. The interpretation of salt addition in those studies is that it induces osmotic stress on the fibrils caused by exclusion of salt from the intermolecular spaces.

The hydrophobic effect

There is increasing evidence that addition of salt can increase hydrophobic interactions in molecular systems (42), which makes sense from entropic considerations when restructuring of water occurs around polar residues. Here, addition of salt to the buffer might be thought to increase interactions among the hydrophobic residues (e.g., proline) among neighboring tropocollagen molecules. The magnitude of this effect is dependent on each ion's ability to be hydrated, known as the Hofmeister series (34), where, for example, ammonium induces a strengthening of the hydrophobic effect, but potassium and sodium do not have such a marked effect. In our study, it is clear that the modulus achieved by adding 1 M salt was irrespective of the cation of the chloride salts. The lack of variation among moduli when different cations were used suggests that this may be a minor effect.

Hydrogen bonding

The role of hydrogen bonding is difficult to assess from these experiments but could be elucidated in the future by substituting water for deuterium oxide (D_20) (43). With an increase in ethanol concentration, the hydrogen bonding among collagen monomers may be expected to change because of displaced water molecules, and would undoubtedly be mediated by hydroxyproline residues. Modulus tuning using water/propanol mixtures has been carried out previously by Radmacher et al. on thin gelatin films on mica, and the modulus increased with increasing alcohol (44). Studies of collagen-based materials, such as dentin, have shown that stiffening and strengthening of the tissue can be attributed to an increase in hydrogen bonding between collagen fibrils (45,46) using different polar solvents.

SUMMARY

Based on discussions in the literature, the most probable interaction forces that control the elastic response of collagen in aqueous conditions can be proposed. When salt concentration or ionic strength is increased, hydration or solvation forces dominate the response. When the pH is lowered, ion pair interactions would seem the most likely to dominate. It is also conceivable that hydrophobic effects play a role in all these scenarios but likely at a lower magnitude than the hydrophilic forces described in each case. A better understanding of which forces modulate the elastic response when one parameter is changed should aid rational design of new materials based on collagen and analogous synthetic peptides. All these effects appear to be fully reversible, which may indicate that it is possible to modulate tissue elasticity in vivo by directed therapeutics, whether the tissue in question is natural or bioengineered implants.

The authors thank Lorna Dougan for useful discussions and Stefan Vinzelberg (Atomic Force, Mannheim, Germany) for assistance in the development of a FV analysis program.

D.J.B. is a White Rose Doctoral Centre lecturer funded by the Engineering and Physical Sciences Research Council. We gratefully acknowledge funding from the Biological Sciences Research Council (BB/D011191/1) and the University of Leeds.

REFERENCES

1. Bozec, L., G. van der Heijden, and M. Horton. 2007. Collagen fibrils: nanoscale ropes. *Biophys. J.* 92:70–75.
2. Yunoki, S., K. Mori, T. Suzuki, N. Nagai, and M. Munekata. 2007. Novel elastic material from collagen for tissue engineering. *J. Mater. Sci. Mater. Med.* 18:1369–1375.
3. Eppell, S. J., B. N. Smith, H. Kahn, and R. Ballarini. 2006. Nano measurements with micro-devices: mechanical properties of hydrated collagen fibrils. *J. R. Soc. Interface.* 3:117–121.
4. Discher, D. E., P. Janmey, and Y.-l. Wang. 2005. Tissue cells feel and respond to the stiffness of their substrate. *Science.* 310:1139–1143.
5. Farrell, E., F. J. O'Brien, P. Doyle, J. Fischer, I. Yannas, et al. 2006. A collagen-glycosaminoglycan scaffold supports adult rat mesenchymal stem cell differentiation along osteogenic and chondrogenic routes. *Tissue Eng.* 12:459–468.
6. Venugopal, M. G., J. A. M. Ramshaw, E. Braswell, D. Zhu, and B. Brodsky. 1994. Electrostatic interactions in collagen-like triple-helical peptides. *Biochemistry.* 33:7948–7956.
7. Gale, M., M. S. Pollanen, P. Markiewicz, and M. C. Goh. 1995. Sequential assembly of collagen revealed by atomic force microscopy. *Biophys. J.* 68:2124–2128.
8. Hodge, A. J., and J. A. Petruska. 1963. Recent studies with the electron microscope on ordered aggregates of the tropocollagen molecule. *In* Aspects of protein structure. G. N. Ramchandaran, editor. Academic Press, New York. 289–300.
9. Ottani, V., D. Martini, M. Franchi, A. Ruggeri, and M. Raspanti. 2002. Hierarchical structures in fibrillar collagens. *Micron.* 33:587–596.
10. Fietzek, P. P., and K. Kühn. 1975. Information contained in the amino acid sequence of the α1(I)-chain of collagen and its consequences upon the formation of the triple helix, of fibrils and crosslinks. *Mol. Cell. Biochem.* 8:141–157.
11. Persikov, A. V., J. A. M. Ramshaw, A. Kirkpatrick, and B. Brodsky. 2005. Electrostatic interactions involving lysine make major contributions to collagen triple-helix stability. *Biochemistry.* 44:1414–1422.
12. Traub, W., and P. P. Fietzek. 1976. Contribution of the α2 chain to the molecular stability of collagen. *FEBS Lett.* 68:245–249.
13. Grant, C. A., D. J. Brockwell, S. E. Radford, and N. H. Thomson. 2008. Effects of hydration on the mechanical response of individual collagen fibrils. *Appl. Phys. Lett.* 92:233902–233904.

14. Heim, A. J., T. J. Koob, and W. G. Matthews. 2007. Low strain nanomechanics of collagen fibrils. *Biomacromolecules*. 8:3298–3301.

15. Heim, A. J., W. G. Matthews, and T. J. Koob. 2006. Determination of the elastic modulus of native collagen fibrils via radial indentation. *Appl. Phys. Lett*. 89:181902–181904.

16. van der Rijt, J. A. J., K. O. van der Werf, M. L. Bennink, P. J. Dijkstra, and J. Feijen. 2006. Micromechanical testing of individual collagen fibrils. *Macromol. Biosci.* 6:697–702.

17. Wenger, M. P. E., L. Bozec, M. A. Horton, and P. Mesquida. 2007. Mechanical properties of collagen fibrils. *Biophys. J*. 93:1255–1263.

18. Yang, L., K. O. van der Werf, C. F. C. Fitie, M. L. Bennink, P. J. Dijkstra, et al. 2008. Mechanical properties of native and cross-linked type I collagen fibrils. *Biophys. J*. 94:2204–2211.

19. Yang, L., K. O. van der Werf, B. F. J. M. Koopman, V. Subramaniam, M. L. Bennink, et al. 2007. Micromechanical bending of single collagen fibrils using atomic force microscopy. *J. Biomed. Mater. Res. A*. 82A:160–168.

20. Kadler, K. E., D. F. Holmes, J. A. Trotter, and J. A. Chapman. 1996. Collagen fibril formation. *Biochem. J*. 316:1–11.

21. Hertz, H. 1881. Uber die Beruhrung fester elastischer Korper (On the contact of elastic solids). *J. Reine Angew. Math*. 92:156–171.

22. A-Hassan, E., W. F. Heinz, M. D. Antonik, N. P. D'Costa, S. Nageswaran, et al. 1998. Relative microelastic mapping of living cells by atomic force microscopy. *Biophys. J*. 74:1564–1578.

23. Grant, C., P. Twigg, A. Egan, A. Moody, A. Smith, et al. 2006. Poly(vinyl alcohol) hydrogel as a biocompatible viscoelastic mimetic for articular cartilage. *Biotechnol. Prog*. 22:1400–1406.

24. Lee, I., and R. E. Marchant. 2000. Force measurements on platelet surfaces with high spatial resolution under physiological conditions. *Colloids Surf. B Biointerfaces*. 19:357–365.

25. Rabinovich, Y., M. Esayanur, S. Daosukho, K. Byer, H. El-Shall, et al. 2005. Atomic force microscopy measurement of the elastic properties of the kidney epithelial cells. *J. Colloid Interface Sci*. 285:125–135.

26. Round, A. N., B. Yan, S. Dang, R. Estephan, R. E. Stark, et al. 2000. The influence of water on the nanomechanical behavior of the plant biopolyester cutin as studied by AFM and solid-state NMR. *Biophys. J*. 79:2761–2767.

27. Schaer-Zammaretti, P., and J. Ubbink. 2003. Imaging of lactic acid bacteria with AFM–elasticity and adhesion maps and their relationship to biological and structural data. *Ultramicroscopy*. 97:199–208.

28. Strasser, S., A. Zink, M. Janko, W. M. Heckl, and S. Thalhammer. 2007. Structural investigations on native collagen type I fibrils using AFM. *Biochem. Biophys. Res. Commun*. 354:27–32.

29. Yang, L., C. F. C. Fitié, K. O. van der Werf, M. L. Bennink, P. J. Dijkstra, et al. 2008. Mechanical properties of single electrospun collagen type I fibers. *Biomaterials*. 29:955–962.

30. Glowacki, J., and S. Mizuno. 2008. Collagen scaffolds for tissue engineering. *Biopolymers*. 89:338–344.

31. Stark, Y., K. Suck, C. Kasper, M. Wieland, M. van Griensven, et al. 2006. Application of collagen matrices for cartilage tissue engineering. *Exp. Toxicol. Pathol*. 57:305–311.

32. Hutter, J. L., and J. Bechhoefer. 1993. Calibration of atomic force microscopy cantilevers. *Rev. Sci. Instrum*. 66:1868–1873.

33. Domke, J., and M. Radmacher. 1998. Measuring the elastic properties of of thin polymer films with the atomic force microscope. *Langmuir*. 14:3320–3325.

34. Hofmeister, F. 1888. About the science of the effect of salts. *Arch. Exp. Pathol. Pharmacol*. 24:247–260.

35. Leikin, S., D. C. Rau, and V. A. Parsegian. 1995. Temperature-favoured assembly of collagen is driven by hydrophilic not hydrophobic interactions. *Nat. Struct. Mol. Biol*. 2:205–210.

36. Parsegian, V. A., R. P. Rand, N. L. Fuller, and D. C. Rau. 1986. Osmotic stress for the direct measurement of intermolecular forces. *Methods Enzymol*. 127:400–416.

37. Israelachvili, J. N. 1991. Intermolecular and Surface Forces, 2nd ed. Elsevier/Academic Press, Amsterdam.

38. Freudenberg, U., S. H. Behrens, P. B. Welzel, M. Muller, M. Grimmer, et al. 2007. Electrostatic interactions modulate the conformation of collagen I. *Biophys. J*. 92:2108–2119.

39. Dick, Y. P., and A. Nordwig. 1966. Effect of pH on the stability of the collagen fold. *Arch. Biochem. Biophys*. 117:466–468.

40. Lindman, S., W.-F. Xue, O. Szczepankiewicz, M. C. Bauer, H. Nilsson, et al. 2006. Salting the charged surface: pH and salt dependence of protein G B1 stability. *Biophys. J*. 90:2911–2921.

41. Leikin, S., D. C. Rau, and V. A. Parsegian. 1994. Direct measurement of forces between self-assembled proteins: temperature-dependent exponential forces between collagen triple helices. *Proc. Natl. Acad. Sci. USA*. 91:276–280.

42. Mancera, R. L. 1998. Does salt increase the magnitude of the hydrophobic effect? A computer simulation study. *Chem. Phys. Lett*. 296:459–465.

43. Dougan, L., A. S. R. Koti, G. Genchev, H. Lu, and J. M. Fernandez. 2008. A single-molecule perspective on the role of solvent hydrogen bonds in protein folding and chemical reactions. *ChemPhysChem*. 9:2836–2847.

44. Radmacher, M., M. Fritz, and P. K. Hansma. 1995. Imaging soft samples with the atomic force microscope: gelatin in water and propanol. *Biophys. J*. 69:264–270.

45. Nalla, R. K., M. Balooch, J. W. Ager Iii, J. J. Kruzic, J. H. Kinney, et al. 2005. Effects of polar solvents on the fracture resistance of dentin: role of water hydration. *Acta Biomater*. 1:31–43.

46. Pashley, D. H., K. A. Agee, R. M. Carvalho, K.-W. Lee, F. R. Tay, et al. 2003. Effects of water and water-free polar solvents on the tensile properties of demineralized dentin. *Dent. Mater*. 19:347–352.